Structural investigation of the ZnSe(001)-$c(2\times2)$ surface

W. Weigand,[1,*] A. Müller,[1] L. Kilian,[1] T. Schallenberg,[2] P. Bach,[2] G. Schmidt,[2] L. W. Molenkamp,[2] O. Bunk,[3]
R. L. Johnson,[4] C. Kumpf,[1] and E. Umbach[1]

[1]*Experimentelle Physik II, Universität Würzburg, Am Hubland, 97074 Würzburg, Germany*
[2]*Experimentelle Physik III, Universität Würzburg, Am Hubland, 97074 Würzburg, Germany*
[3]*Materials Research Department, Risø National Laboratory, Frederiksborgvej 399, DK-4000 Roskilde, Denmark*
[4]*Institut für Experimentalphysik, Universität Hamburg, Luruper Chausse 149, D-22761 Hamburg, Germany*
(Received 13 August 2003; published 31 December 2003)

Zinc selenide is a model system for II-VI compound semiconductors. The geometric structure of the clean (001)-$c(2\times2)$ surface has recently been the subject of intense debate. We report here a surface x-ray-diffraction study on the ZnSe(001)-$c(2\times2)$ surface performed under ultrahigh vacuum using synchrotron radiation which reveals the precise atomic geometry. The results are in excellent agreement with the Zn-vacancy model proposed earlier on the basis of density-functional theory calculations and unequivocally establish the correct equilibrium surface structure.

The field of II-VI compound semiconductors has attracted considerable interest recently due to important progress in the fabrication of electronic and optoelectronic devices[1–3] and, in particular, due to the injection of spin-polarized electrons into nonmagnetic semiconductors (see, e.g., Refs. 4 and 5, and references therein) which was achieved by alloying II-VI semiconductor thin films with a magnetic material such as Mn. Since interface effects are often important in thin-film systems a good knowledge of the electronic and geometric structures of surfaces and interfaces is indispensable for device design optimization. For example, to achieve high-quality pseudomorphic growth of II-VI compound thin films on III-V substrates a detailed knowledge about the II-VI/III-V interface and the II-VI surface is essential. An example for recent progress in this field is the $c(2\times2)$-reconstructed ZnSe(001) surface. Marangolo *et al.* reported interesting magnetic properties induced by one monolayer of Fe on this surface.[6,7] However, there is still an ongoing discussion concerning the exact geometric structure of the clean $c(2\times2)$-reconstructed ZnSe(001) surface which is somewhat surprising since this system has been extensively investigated in the past and is considered to be a model system for II-VI molecular beam epitaxy (MBE) growth.

The structural models described in the literature for the ZnSe(001) surface contain dimers or atomic vacancies at the surface.[8–14] Most of the structural studies performed on the $c(2\times2)$ reconstruction in the last decade[8,13,14] favor the Zn-vacancy model shown in Fig. 1(a) which is also supported theoretically.[9,10] But reflection high energy electron diffraction (RHEED) rocking curve investigations of Ohtake *et al.*[12] on both the (2×1) and $c(2\times2)$-reconstructed ZnSe(001) surfaces cast doubt on the conventional wisdom; a Se-vacancy model [Fig. 1(b)] describes samples during the atomic layer epitaxy growth process. The Se-vacancy model is very similar to the Zn-vacancy model but the Zn and Se atoms are swapped and the atoms near the surface have very different relaxations. The similarity of the atomic positions makes it difficult to distinguish between the two different vacancy models using techniques which lack chemical specificity. Since the electron densities of Zn and Se are similar

this generally also applies to surface x-ray diffraction (SXRD). However based on the different surface relaxations predicted by density-functional theory (DFT) calculations[9] it is possible to identify the correct model from our SXRD results.

The samples were grown in a combined III-V/II-VI MBE system at the University of Würzburg using standard techniques. On an undoped GaAs(001) buffer layer a 165-nm-thick ZnSe film[15] was deposited at a substrate temperature of 320 °C. Cooling the samples under Zn flux produces a $c(2\times2)$-reconstructed surface. Subsequently the samples were capped by a protective amorphous Se layer to avoid surface contamination and were transported to HASYLAB under ultrahigh vacuum (UHV) conditions ($p<10^{-9}$ mbar) using a mobile UHV shuttle. The final surface preparation was performed by desorption of the Se cap and annealing the surface at a temperature of 400 °C. This procedure recovers a $c(2\times2)$-reconstructed surface with an average domain size of up to 800 Å.[15] Afterwards the sample was transferred into a portable UHV chamber with a hemispherical Be window which was mounted at the z-axis diffractometer at the BW2 wiggler beam line at HASYLAB. The sample surface was
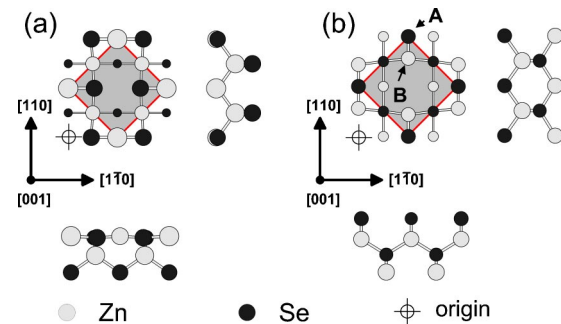

FIG. 1. (Color online) Schematics of (a) the Zn-vacancy and (b) the Se-vacancy models derived from DFT calculations (Refs. 9 and 10). The reduced $c(2\times2)$ unit cell is shown as a gray area. Smaller circles indicate atoms in deeper layers. A top view (along $[00\bar{1}]$) and side views (along $[110]$ and $[1\bar{1}0]$, respectively) are shown in each case.
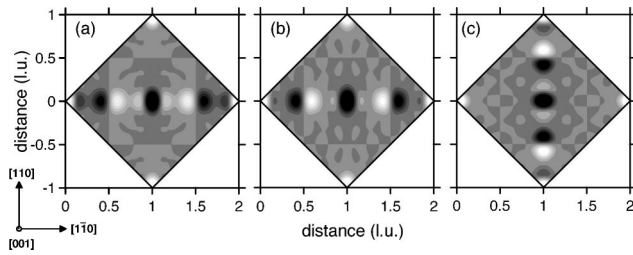
FIG. 2. Two-dimensional maps of the Patterson functions calculated from (a) our measured fractional-order in-plane data, (b) from the Zn-vacancy, and (c) from the Se-vacancy models (Ref. 9). Positive peaks (white color coding) correspond to atomic distance vectors within the reduced $c(2 \times 2)$ unit cell, negative peaks are induced by omitting the integer order data (see text). Axes are scaled in LEED units.

then aligned with respect to the incidence beam. A full data set was recorded using a wavelength of 1.305 Å and a grazing incidence angle of 0.35°. The intensity $|F_{hkl}|^2$ (where F_{hkl} is the structure factor) of the reflection (hkl) was determined by rotating the sample about its surface normal (ω scan). The peaks were integrated, background subtracted, and corrected for Lorentz and polarization factors, active sample area, and rod intercept in the standard manner.[16,17] The diffraction pattern revealed a $c2mm$ symmetry. By averaging symmetry-equivalent reflections of the in-plane data set a systematic error in $|F|^2$ of $\epsilon = 12.4\%$ was determined. The final data set consisted of 40 nonequivalent in-plane reflections, 9 fractional-order rods with 324 reflections, and 4 crystal truncation rods with 156 reflections. For fitting the data we used the code "fit."[18] In the following discussion standard low-energy electron-diffraction (LEED) coordinates $(\vec{a} = \frac{1}{2}[1\bar{1}0]_{\text{bulk}}, \vec{b} = \frac{1}{2}[110]_{\text{bulk}}, \vec{c} = [001]_{\text{bulk}})$ are used.

Usually the first step in a structure determination by SXRD is an analysis of the so-called Patterson function which immediately reveals interatomic distance vectors in the surface structure. The two-dimensional Patterson function $P(xy) \propto \Sigma_{h,k} |F_{hk0}|^2 \cos[2\pi(hx + ky)]$ is either calculated using the *in-plane* structure factors F_{hk0} obtained from the measurement (for the *experimental* Patterson function) or calculated from a certain atomic model (for the *theoretical* Patterson function). Figure 2(a) shows the map of the experimental Patterson function obtained from our data while (b) and (c) represent theoretical Patterson functions calculated for the Zn-vacancy and the Se-vacancy models, respectively.[9] Since only *fractional*-order in-plane data were used the two-dimensional-Patterson map shows the differences between the surface reconstruction and the bulk. Positive peaks in the maps identify interatomic distance vectors in the reconstruction. Negative peaks in the maps are artificially produced by omitting the integer order data.[19] Only two *inequivalent* positive peaks are visible in the experimental Patterson map [Fig. 2(a)] at $(0.60, 0)$ and $(0.83, 0)$, all others are due to the unit-cell symmetry. As will be discussed below they correspond to Zn-Se and Se-Se interatomic distance vectors in the surface plane. These peaks are reproduced best by the theoretical Patterson map for the Zn-vacancy model [Fig. 2(b)]. However it should be noted that
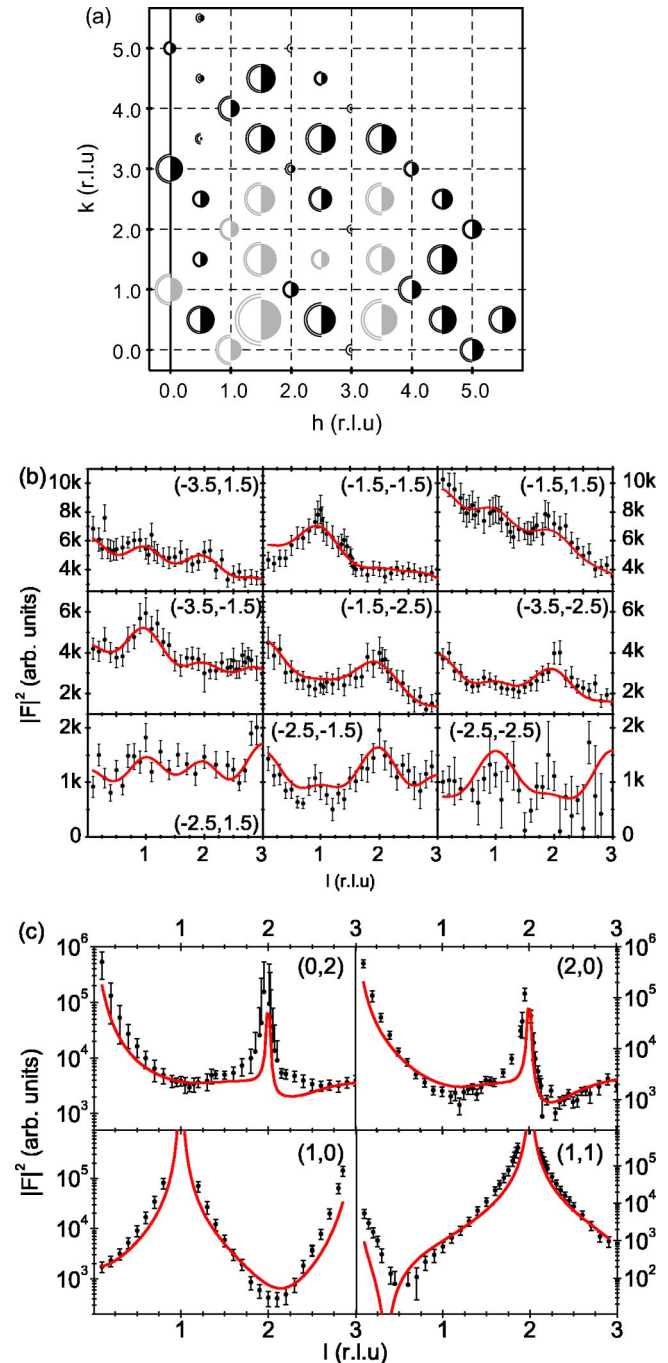

FIG. 3. (Color online) Plot of the final fit (see Fig. 4 and Table I) and the measured data. (a) In-plane data: The areas of the open and filled semicircles represent measured and calculated intensities. Gray/white circles have been scaled by a factor 0.5 with respect to the black/white circles. (b) Fractional- and (c) integer-order rods: Error bars and solid lines represent the measured and calculated data, respectively.

the Se-vacancy model [Fig. 2(c)] might also explain the experimental Patterson map. When Fig. 2(a) is rotated by 90° (which might be allowed since it is difficult to distinguish between the [110] and the [1$\bar{1}$0] directions in the experiment) it compares quite well with Fig. 2(c) with one small difference, namely, the change of the positions of the mini-
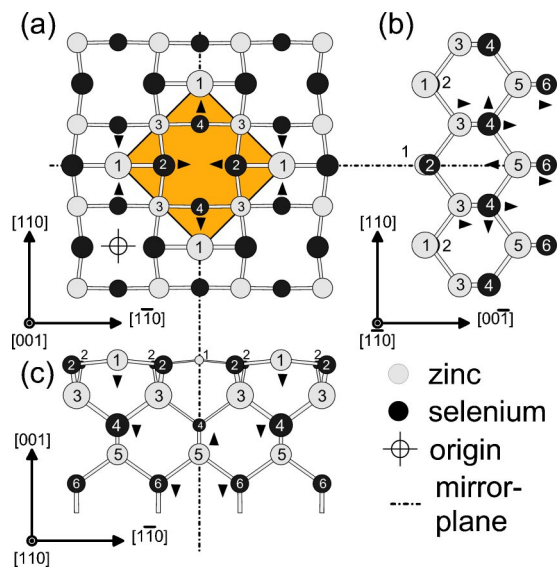
FIG. 4. (Color online) Structural model for the ZnSe(001)-c(2 ×2) surface viewed (a) from the top, (b) and (c) from the side. Gray bars represent covalent bonds. The reduced c(2×2) unit cell is shown as a gray area. Small arrows indicate the direction of relaxation of the atoms. Dash-dotted lines indicate mirror planes.

mum at (0,0.41) and the maximum at (0, 0.59). This may be explained by a slightly different atomic arrangement, namely, a smaller lateral distance between Zn and Se atoms in the uppermost bilayer. In conclusion the analysis of the Patterson maps confirms the presence of a vacancy site and favors Zn rather than Se vacancies.

In order to identify the correct model we performed several refinement runs for both the Zn- and the Se-vacancy models. Atomic positions, Debye-Waller factors, and occupancies of several atomic layers of the model were varied in order to minimize the difference between measured and calculated intensities in a standard least-squares-fit routine.[17] In a first series of fits performed on the Zn-vacancy model the atomic positions of an increasing number of atomic layers were refined ending in a fit of three ZnSe bilayers (atoms 1–6 in Fig. 4) which resulted in $\chi^2=2.39$ for the complete data set. Including more than three bulk layers in the refinement increased χ^2 due to the larger number of fit parameters. Subsequently isotropic Debye-Waller (DW) factors for each individual atom in the first two bilayers and two bulk DW values were varied which reduced χ^2 to 1.57, a reasonable small value. Another series of fits in which the occupancy of the surface atoms was varied revealed that all atomic sites in the model are fully occupied. In the following we discuss the final fit which is shown in Fig. 3. The corresponding model is illustrated in Fig. 4 and all fit-parameters are listed in Table I.

As demonstrated in Fig. 3(a) the in-plane data and the fractional-order rods are very well reproduced by the final Zn-vacancy model. The integer order rods which are an important part of the SXRD data set since they contain the information about the registry between the surface structure and the bulk show some deviations which are visible mainly close to the bulk Bragg points. Beside the fact that integer order SXRD data in general are difficult to fit since the entire surface including disordered or unreconstructed areas contributes to their intensity another possible explanation for the discrepancy in our case is the small thickness of the ZnSe layer of 165 nm. As the measurements were performed at a grazing incidence angle of 0.35° above the critical angle for total reflection of 0.26° the penetration depth was much larger than the thickness of the ZnSe film. Therefore the ZnSe layer *and* the GaAs bulk crystal contribute to the integer order intensities, a fact which cannot be taken into account by our model. However for the fractional-order the intensity arises uniquely from the c(2×2) reconstruction. Thus the fit to the fractional-order data yields atomic positions which are not influenced by the GaAs substrate. Such a fit gave $\chi^2=1.10$, an excellent value, and yielded atomic positions which are—within the error bars given in Table I—identical to the best fit of the Zn-vacancy model described above. This confirms that the derived model is in excellent agreement with the data despite the imperfect reproduction of the integer-rod data due to the finite ZnSe layer thickness.

The Zn-vacancy model consists of half a monolayer of Zn atoms (called the adlayer in the following) on the (001) surface of a Se-terminated ZnSe bulk crystal. The most remarkable structural feature of the refined Zn-vacancy model is the fact that the Zn ad-layer is almost completely pulled into the plane of the uppermost Se layer [see Fig. 4(c)]. This strong vertical relaxation is illustrated by the height difference between the Zn adatoms (1 in Fig. 4) and the uppermost Se

TABLE I. Atomic parameters of the Zn-vacancy model. Column 2 details the isotropic Debye Waller (DW) factors in Å^2 (SXRD results). DW factors for the atoms 5 Zn and 6 Se (and in deeper layers) were fixed at bulk values. Columns 3 and 4 show LEED coordinates of the atoms obtained from SXRD and DFT, respectively. Standard deviations were calculated assuming uncorrelated parameters. Positions without error were not refined due to $c2mm$ symmetry constraints. In the DFT calculations only the atomic positions 1–3 were refined. Column 5 contains the deviations between both methods in angstroms.

		DW	Positions (SXRD)			Positions (DFT) (Ref. 9)			Difference (Å)		
1	Zn	3.64(7)	1	0	−0.208(4)	1	0	−0.2312	0	0	0.132
2	Se	1.33(2)	0.557(1)	1	−0.240(4)	0.5588	1	−0.2470	−0.007	0	0.040
3	Zn	1.98(2)	1.5	0.5	−0.499(2)	1.5	0.5	−0.5016	0	0	0.015
4	Se	0.75(2)	1	0.494(1)	−0.753(2)	1	0.5	−0.75	0	−0.024	−0.017
5	Zn	1.2	1	1	−0.996(2)	1	1	−1	0	0	0.023
6	Se	0.60	0.502(1)	1	−1.251(1)	0.5	1	−1.25	0.008	0	0.006

atoms (2) of only 0.18 Å. The bulklike height difference between a Zn- and a Se-layer is 1.42 Å. As a consequence the Se atoms (2) are pushed away laterally from their bulk positions. The atomic shifts are illustrated by small arrows in Fig. 4. All bond distances are very close to the sum of the covalent radii of Zn and Se (2.45 Å). The distance between the Zn adatoms (1) and the uppermost Se atoms (2) is 2.23 Å and corresponds to the maximum at (0.60, 0) in the Patterson function mentioned above [see Fig. 2(a)]. The bond length between atoms 2 and 3 (2.49 Å) is even closer to the covalent bond length. The second peak in the Patterson function at (0.83, 0) corresponds to the distance of 3.53 Å between the Se atoms in the top layer (2). The atomic positions obtained from our SXRD analysis are in very good agreement with the positions calculated by Park and Chadi[9] (see Table I). The z coordinate of the Zn adatom differs by only 0.13 Å which is a small value compared to the shift of the atom from its bulklike position (1.18 Å). For all other atoms the deviations are below 0.04 Å.

Despite the very good agreement of SXRD and DFT results for the Zn-vacancy model it is not clear *a priori* that the Se-vacancy model can be excluded. Since the atomic numbers of Zn and Se are very similar it is impossible to distinguish the atoms in a conventional x-ray-diffraction experiment. In other words a model with the same atomic positions but with the atomic species exchanged would result in a fit of similar quality. However the fact that the ad-atoms are pulled into the surface of the ZnSe crystal is an important result of our fitting procedure and allows to identify the correct model. For the Se-vacancy models (for both by Park and Chadi[9] and by Ohtake *et al.*[12]) the atomic configurations in the ad-layer and in the uppermost bulk layer differ from those of the Zn-vacancy model not only by an exchange of

Zn and Se atoms, but also by the fact that the ad-atoms (Se in this case) are *not* pulled into the surface. The key features of the Se-vacancy models are a large *height difference* of 1.65 Å between the uppermost Se and Zn atoms, and consequently a reduced *lateral distance* between them [the atoms are labeled A and B in Fig. 1(b)]. These characteristics are in contradiction to our experimental finding. The reduced lateral distance disagrees with the experimental Patterson function (see above) and the bulklike height of the Se-atom could not be verified in the fitting procedure: When the Se-vacancy model is used as a starting model for the data analysis a relatively small χ^2 of 1.93 is obtained by the refinement but the final arrangement is very similar to the Zn-vacancy model with the two atoms exchanged. In particular the Se ad-atoms are shifted downwards to almost the same level as the first bulklike Zn layer. This represents a characteristic feature of the $c(2 \times 2)$ reconstruction and provides clear evidence that the Zn-vacancy model is the correct description of the ZnSe(001) surface.

In summary we have performed a study of the $c(2 \times 2)$-reconstructed ZnSe(001) surface using surface x-ray diffraction, and presented a detailed structural model with rather accurate geometric parameters. Despite recent suggestions to the contrary we find that the equilibrium $c(2 \times 2)$-surface structure is best described by the Zn-vacancy model.

---

*Electronic address: weigand@dix.physik.uni-wuerzburg.de

[1] S.V. Ivanov, Phys. Status Solidi A **192**, 157 (2002).

[2] S.V. Ivanov, A.A. Toropov, T.V. Shubina, S.V. Sorokin, O.V. Nekrutkina, V.A. Kaygorodov, P.S. Kopev, G. Reuscher, M. Keim, A. Waag, and G. Landwehr Phys. Status Solidi A **180**, 275 (2000).

[3] K. Sato, T. Asahi, M. Hanafusa, A. Noda, A. Arakawa, M. Uchida, O. Oda, Y. Yamada, and T. Taguchi Phys. Status Solidi A **180**, 267 (2000).

[4] R. Fiederling, M. Keim, G. Reuscher, W. Ossau, G. Schmidt, A. Waag, and L.W. Molenkamp, Nature (London) **402**, 787 (1999).

[5] P. Grabs, G. Richter, R. Fiederling, C.R. Becker, W. Ossau, G. Schmidt, L.W. Molenkamp, W. Weigand, E. Umbach, I.V. Sedova, and S.V. Ivanov Appl. Phys. Lett. **80**, 3766 (2002).

[6] M. Marangolo, G.M. Guichar, M. Eddrief, and V.H. Etgens Phys. Rev. B **63**, 153302 (2001).

[7] M. Marangolo, F. Gustavsson, M. Eddrief, P. Sainctavit, V.H. Etgens, V. Cros, F. Petroff, J.M. George, P. Bencok, and N.B. Brookes Phys. Rev. Lett. **88**, 217202 (2002).

[8] W. Chen, A. Kahn, P. Soukiassian, P.S. Mangat, J. Gaines, C. Ponzoni, and D. Olego Phys. Rev. B **49**, 10 790 (1994).

[9] C. Park and D. Chadi, Phys. Rev. B **49**, 16 467 (1994).

[10] A. Garcia and J.E. Northrup, J. Vac. Sci. Technol. B **12**, 2678 (1994).

[11] A. Garcia and J.E. Northrup, Appl. Phys. Lett. **65**, 708 (1994).

[12] A. Ohtake, T. Hanada, T. Yasuda, K. Arai, and T. Yao, Phys. Rev. B **60**, 8326 (1999).

[13] H.H. Farrell, M.C. Tamargo, S.M. Shibli, and Y. Chang, J. Vac. Sci. Technol. B **8**, 884 (1990).

[14] Z.H. Chen, M. Sokolowski, F. Stadler, M. Schneider, R. Fink, and E. Umbach, Europhys. Lett. **59**, 552 (2002).

[15] W. Weigand, C. Kumpf, M. Sokolowski, A. Bader, C. Schumacher, A. Möginger, W. Faschinger, L.W. Molenkamp, and E. Umbach Phys. Status Solidi B **229**, 117 (2002).

[16] E. Vlieg, J. Appl. Crystallogr. **30**, 532 (1997).

[17] R. Feidenhans'l, Surf. Sci. Rep. **10**, 105 (1989).

[18] O. Bunk (unpublished).

[19] J. Bohr, R. Feidenhans'l, M. Nielsen, M. Toney, R.L. Johnson, and I.K. Robinson, Phys. Rev. Lett. **56**, 2878 (1986).